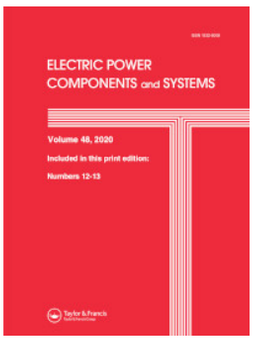

Taylor & Francis
Taylor & Francis Group

Electric Power Components and Systems

ISSN: (Print) (Online) Journal homepage: https://www.tandfonline.com/loi/uemp20

Performance Evaluation of Power Differential and Sensitivity Based Protection for Active Distribution Systems

Patrick T. Manditereza & Ramesh C. Bansal

To cite this article: Patrick T. Manditereza & Ramesh C. Bansal (2020) Performance Evaluation of Power Differential and Sensitivity Based Protection for Active Distribution Systems, Electric Power Components and Systems, 48:12-13, 1378-1389, DOI: 10.1080/15325008.2020.1854389

To link to this article: https://doi.org/10.1080/15325008.2020.1854389

Electric Power Components and Systems, 48(12-13): 1378–1389, 2020

ISSN: print / online
DOI: 10.1080/15325008.2020.1854389

Performance Evaluation of Power Differential and Sensitivity Based Protection for Active Distribution Systems

Patrick T. Manditereza[1] and Ramesh C. Bansal[2]
[1]Department of Electrical, Electronic and Computer Engineering, Central University of Technology, Free State, South Africa
[2]Department of Electrical Engineering, University of Sharjah, Sharjah, United Arab Emirates

CONTENTS

1. Introduction
2. Operation of the Active Power Differential and Sensitivity Analysis (APdSA) Algorithm
3. Performance Evaluation of the APdSA Protection Algorithm
4. Results and Discussion
5. Conclusion
References

Abstract—Protection performance is characterized by qualities that include selectivity, speed, sensitivity and stability. Generally, selectivity and speed present conflicting requirements on the protection design, as do sensitivity and stability requirements. The integration of distributed generation (DG), in particular at the distribution level, further compromises satisfactory achievement of these performance qualities. A recent paper by the authors introduced a protection algorithm based on active power differential and sensitivity analysis (APdSA) for the protection of active distribution systems and microgrids. This paper investigates the performance characteristics of this algorithm with respect to selectivity, sensitivity, stability, and speed. It is shown that, with an important modification to the protection zoning arrangement, the APdSA algorithm is able to selectively clear faults in a DG-integrated distribution system with high sensitivity, stability, and speed, with more than 95% reach over a wide range of fault resistances. The algorithm is also tolerant to communication failure.

Keywords: protection algorithm, voltage based protection, wide area protection, distribution system protection, microgrid protection, fault detection algorithms, impact of distributed generation, protection performance characteristics, sensitivity analysis, power differential based protection

Received 9 December 2019; accepted 1 November 2020

Address correspondence to Patrick T. Manditereza, Department of Electrical, Electronic and Computer Engineering, Central University of Technology, Free State, South Africa. E-mail: pmandite@cut.ac.za

1. INTRODUCTION

Protection systems play an important role in the delivery of electrical power from generating stations to consumers. No matter how well designed a power network is, faults will always occur [1] and protection must be installed to ensure the power is delivered safely and reliably. The protection must be sensitive in order to detect the smallest of fault, ideally in the incipient stage. The protection must also ensure isolation of only the faulted equipment or minimum area in order to ensure power is not disrupted to the majority of consumers. This means the protection must be selective in its operation. This is achieved by dividing the power network into zones and the protection must operate to isolate only the zone in which the fault has occurred. This in turn requires that the protection must be stable and not operate for out-of-zone faults. Once the fault is detected it

must be removed quickly so that damage to equipment and risk to power system stability is minimized.

The protection must, thus, exhibit the performance qualities of speed, selectivity, sensitivity and stability [2]. However, these qualities present conflicting requirements on the design of the protection and it could be difficult to achieve correct balance between the required sensitivity and stability [1], [3]. For instance, high sensitivity may lead to instability [3], [4]. Fast relay operation may also lead to loss of selectivity, and this is especially the case with time-current based protection systems that are traditionally used on the distribution system. The sequence of the time-graded protection devices is designed to ensure that only those relevant to the faulty zone complete the tripping function [5]. The other devices then reset. This means the protection must be intentionally delayed in order to achieve selectivity. Similarly, the sensitivity needs to be reduced so that the protection does not inadvertently trip for out-of-zone faults.

In contrast, unit protection schemes used for the protection of important components and feeders, respond only to faults occurring within the respective zone, thereby achieving high speed operation that is also very selective [6]. However, due to various constraints, the sensitivity of the unit protection schemes cannot be set below a certain minimum level. For example, in a current differential scheme line charging currents may cause significant differences between the currents at the two ends of the line in the absence of fault [6]. Similarly, due to the presence of some false differential currents [7], the minimum required differential relay pick-up settings mean that the transformer or generator differential protection, for example, is not able to protect the entire winding [1]. Protection systems working on different principles may be added to compliment the differential scheme and provide protection for the entire winding [1].

The integration of distributed generators (DGs) has been shown to affect the short circuit current magnitudes and direction of flow impacting the sensitivity and stability of the protection schemes leading to possible loss of selectivity, especially at the distribution level [8], [9]. Hence, new protection strategies are required that can selectively remove faults in a distribution grid with distributed architecture.

In a recent paper [10], the authors introduced a protection algorithm based on active power differential and sensitivity analysis (APdSA) for the protection of active distribution systems and microgrids. The APdSA algorithm is applied over a protection zone that includes a busbar and all feeders terminating at that node as explained in [11], and referred to as Busbar Area Protection (BAP) zone. The algorithm identifies a BAP zone over which it monitors power flows. Some sensitivity-based fault detection indices (FD-Indices) were identified that are generated when a fault occurs within the respective BAP zone. The algorithm is able to identify the faulted zone and subsequently, through peer-to-peer communications with IEDs at neighboring nodes, the specific faulted node or feeder in that zone. An attribute of the APdSA algorithm that is not comparable to any existing protection is that it is reconfigurable and provides economy by requiring only one primary relay at a node irrespective of the number of feeders terminating at that node.

This paper investigates the performance characteristics of the APdSA algorithm. The performance is evaluated with respect to selectivity, sensitivity, stability and speed of operation. Other factors that impact the performance of protection systems, such as fault resistance and communication failure, are also investigated. The major contribution of this paper lies in the modification to the BAP zone that excludes the load (or generator) from the protection zone, removing the impact of load and generation variations on the sensitivity of the APdSA algorithm. This makes protection based on the APdSA algorithm extremely sensitive with pick-up setting of close to zero. This improved sensitivity extends the reach of the APdSA algorithm to cover more than 95% of the protected line, over a wider range of fault resistances. The results from this study also show that the APdSA algorithm is able to concurrently improve the protection performance qualities of sensitivity, stability, selectivity and speed which traditionally have been shown to present conflicting requirements on the design of the protection, and is tolerant to communication failure.

The remainder of this paper is organized as follows: Section 2 analyses the operation of the APdSA algorithm. Section 3 discusses the approach followed for the evaluation of the performance of the APdSA algorithm. The performance of the algorithm is demonstrated and discussed in Section 4. Conclusions are drawn in Section 5.

2. OPERATION OF THE ACTIVE POWER DIFFERENTIAL AND SENSITIVITY ANALYSIS (APDSA) ALGORITHM

2.1. Fault Detection (FD) Indices

The APdSA algorithm achieves its protection function through power flow and sensitivity calculations over a BAP protection zone that includes a busbar and all feeders

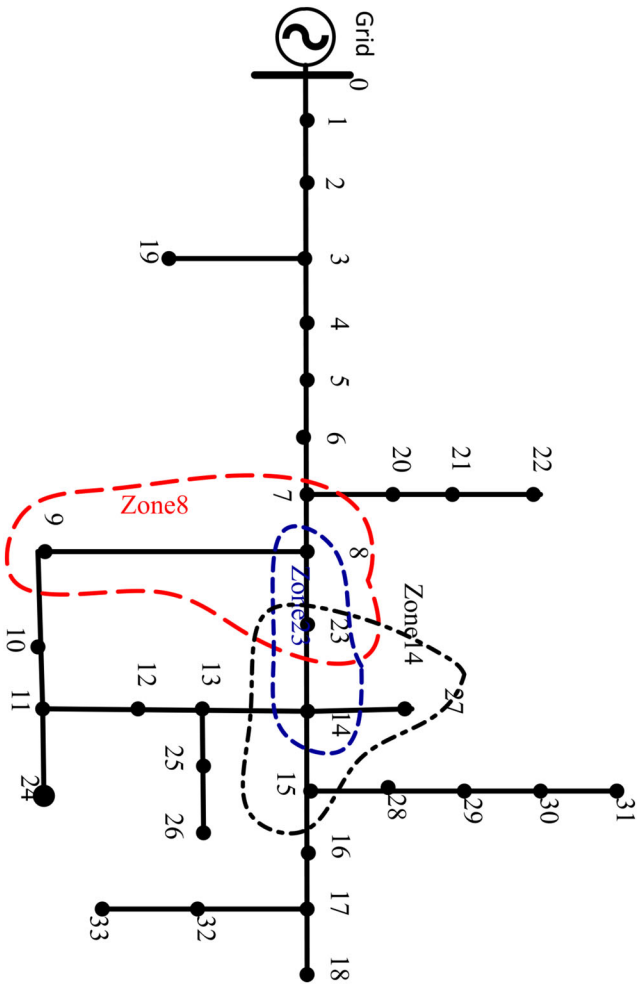

FIGURE 1. Modified IEEE 34-node test system based on the concepts proposed by Mandidereza and Bansal, 2018.

terminating at that node. Some of these BAP zones, identified as Zone8, Zone14 and Zone23, are shown in the modified IEEE 34 node test network in Figure 1. This network is described in [12] and is used for the study presented in this paper. The line and load data for the network is also given in [13]. Three distributed generators (DGs) are installed at nodes 21, 27 and 30. The DG ratings are given in [10].

The changes in node voltage in a network are related to the power flow changes by equation (1) [14]:

$$\begin{bmatrix}\Delta P\\ \Delta Q\end{bmatrix} = \begin{bmatrix}\frac{\partial P}{\partial \delta} & \frac{\partial P}{\partial V}\\ \frac{\partial Q}{\partial \delta} & \frac{\partial Q}{\partial V}\end{bmatrix}.\begin{bmatrix}\Delta\delta\\ \Delta V\end{bmatrix} = [\ J\ ].\begin{bmatrix}\Delta\delta\\ \Delta V\end{bmatrix} \quad (1)$$

where [J] is the Jacobian matrix.

Sensitivity based fault detection indices (FD-Indices) were derived from the Jacobian matrix of the network segment formed by each BAP zone. The FD-Indices at node k of a BAP zone with n nodes are given by [10],

$$C_{k,P} = -\left(\frac{S_{V,P.}}{S_{V,Q}}\right)\Delta P_k \quad (2)$$

$$C_{k,F} = \left(\frac{\Delta V_k - V_{D,k}}{S_{V,Q}}\right)\left(\frac{S_{V,P.}}{S_{V,Q}}\right)\Delta P_k \quad (3)$$

where,

$$S_{V,P} = M^{-1}N^{-1};\ \ S_{V,Q} = -M^{-1}T^{-1}$$
$$V_{D,k} = -(M^{-1}N^{-1}R - M^{-1}T^{-1}U)$$

and,

$$M = \left[\left(\frac{\partial P_k}{\partial \delta_k}\right)^{-1}\left(\frac{\partial P_k}{\partial V_k}\right) - \left(\frac{\partial Q_k}{\partial \delta_k}\right)^{-1}\left(\frac{\partial Q_k}{\partial V_k}\right)\right];$$
$$N = \frac{\partial P_k}{\partial \delta_k};\ \ T = \frac{\partial Q_k}{\partial \delta_k};$$
$$R = \left(\sum_{\substack{j=1\\ j\neq k}}^{n}\frac{\partial P_k}{\partial \delta_j}\Delta\delta_j + \sum_{\substack{j=1\\ j\neq k}}^{n}\frac{\partial P_k}{\partial V_j}\Delta V_j\right);$$
$$U = \left(\sum_{\substack{j=1\\ j\neq k}}^{n}\frac{\partial Q_k}{\partial \delta_j}\Delta\delta_j + \sum_{\substack{j=1\\ j\neq k}}^{n}\frac{\partial Q_k}{\partial V_j}\Delta V_j\right)$$

where P_k, Q_k, V_k, and δ_k are respectively the active power, reactive power, voltage magnitude and angle at node k; Y_{kj} and δ_{kj} are the magnitude and argument of the element (k, j) in the BAP segment's admittance matrix.

Equations (2)–(3) give the FD-Indices $C_{k,P}$ and $C_{k,F}$ on which the APdSA algorithm is based. As can be deduced from (2)-(3), the algorithm is sensitive to real (active) power flow changes (ΔP_k) only and is not impacted by changes to reactive power flows (ΔQ_k). The FD-Indices $C_{k,P}$ and $C_{k,F}$ are calculated at each node of the network. The algorithm requires, as inputs, the synchronized (PMU) measurements of the fundamental voltage magnitude and phase at the 'home' node k (where the relay is located), as illustrated in Figure 2a, and at the nodes at the remote ends of the feeders [10] through reliable communication channels [15]. FD-Indices with positive magnitude are generated when a fault occurs within the respective BAP zone. The FD-Indices at nodes that are outside the faulted zone have zero or negative magnitude.

From (2)-(3) it is obvious that normal load changes also generate $C_{k,P}$ and $C_{k,F}$ of certain magnitude. In [10] it was shown that short circuits generated FD-Indices that were much larger than those due to maximum change in load, which is when the maximum load is switched in. The load therefore imposed a limit on the sensitivity that could be

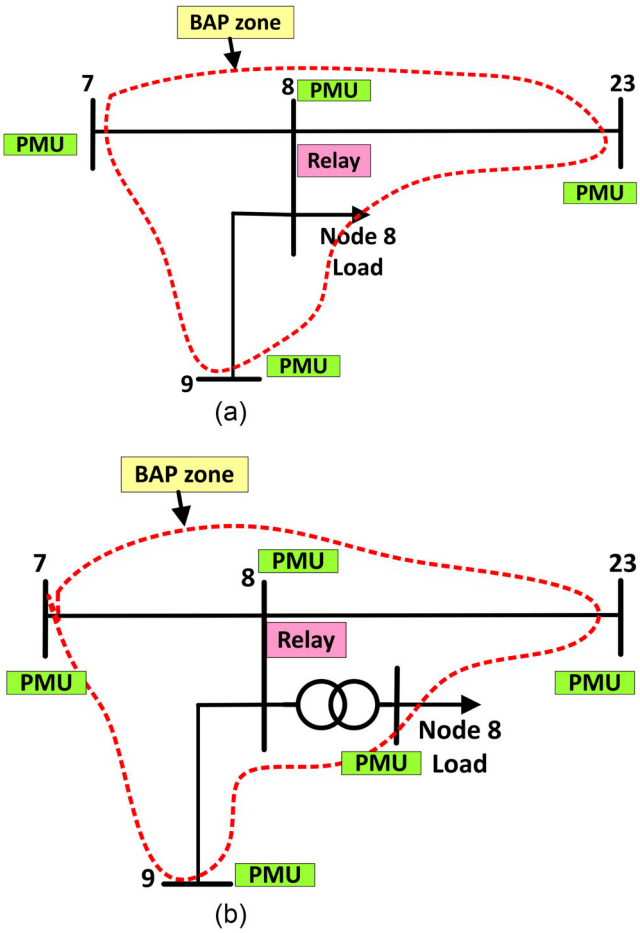

FIGURE 2. Node 8 BAP zone, (a) The load inside the BAP zone, and (b) Modified BAP zone with load external to the zone.

achieved. In this paper, the sensitivity of the algorithm is improved by modifying the BAP zone. In [10] the load was included in the protection zone hence generating the FD-Indices under normal operating conditions. In the present work, therefore, the loads are removed from the protection zone. This is achieved by placing an additional PMU at the secondary terminals of the load transformer, as illustrated in Figure 2b, with the load transformer itself remaining within the protection zone. Normal load changes are therefore not visible to the algorithm meaning ΔP_k is zero and appears only under fault conditions. The pick-up threshold for $C_{k,P}$ and $C_{k,F}$ can thus be set to zero. A similar re-arrangement is done at the generator nodes – the generator transformer is placed within the protection zone but with the generator itself external to the zone. Changes to the generation therefore do not impact the power flow balance within the BAP zone.

Inclusion of the transformer in the BAP zone needs special consideration. The APdSA protection algorithm performs calculations in the per unit system, hence, the transformers are replaced by the equivalent reactance. The additional phase shift between the primary and secondary voltages resulting from the transformer winding connections needs to be included in the argument δ_{kj} of the transformer element in the BAP segment's admittance matrix.

The use of measurements from multiple locations gives the APdSA algorithm features of unit protection, enabling the algorithm to have an overall view of the protected system, thus overcoming the shortcomings of traditional OC protection and is able to isolate faults quickly. OC protection uses only local measurements and is time-graded to achieve coordination which may lead to long fault clearance times. Impedance (or distance) based protection also uses single-point measurements, but can clear faults quickly using information received from the remote end. As noted above, the pick-up of the APdSA relay can be set to zero. That is, the sensitivity of the algorithm is not limited by load current. This contrasts with the traditional overcurrent (OC) protection that is designed to pick-up for faults above full load current. The APdSA is being proposed as an alternative to OC protection in DG-integrated distribution systems and thus offers a more sensitive and faster option. Impedance protection has also been proposed for application to the DG-integrated distribution system but its sensitivity is also impacted by the load current, due to load encroachment, and impedance measurement errors due to current in-feeds, which is a result of single-point measurements [16]. Current differential protection is another alternative. However, the minimum setting current is limited by the line charging current thereby reducing the sensitivity of the protection [6] [17].

Various protection techniques have been proposed by other researchers that use multi-point measurements from PMUs. The work reported in [17] [18] implements the simple current differential scheme but using wide area measurement systems (WAMS) in order to overcome the problems associated with conventional implementation of current differential protection on long lines. Most of the proposed techniques, though, use a centralized architecture and are aimed at providing wide area backup protection. The researchers in [16] [19] propose a current differential scheme that utilizes wide area current data from PMUs located at several busbars, a fault being indicated when the sum of zero- and/or positive-sequence currents entering the protected zone increases beyond a specified threshold. The work in [20] applies Clarke transformation on the measured synchronized voltage and current phasors to generate some fault detection indices. The authors in [21] proposes

the use of a fault index which is similar in concept to the Lyapunov exponent (LE). The index is calculated centrally using the frequencies received from the PMUs across the selected system. The work reported in [22] proposes a method that uses fault detection indices based on network power flows to identify transmission line faults. The works reported in [23] [24] employ a centralized approach to determine the fault zone, faulted busbar and faulted line, in that order, using an optimized number of PMUs. The work presented in [25] follows a similar approach but uses reactive power flows on lines terminating at a busbar to identify the faulted transmission line. As can be deduced from the above, most of the published papers propose fault detection algorithms that use both voltage and current phasors. The APdSA algorithm however, provides a different approach that uses only voltage phasors. This approach is suitable for the emerging DG-integrated distribution system operating environment in which the fault current magnitudes may not be predictable. In fact, the fault currents may differ little from normal load currents in distribution systems integrated with mostly inverter-interfaced DGs [26].

2.2. Operation of the APdSA Algorithm

When a single phase to ground fault occurs at node 7 of the study network in Figure 1, positive $C_{k,P}$ and $C_{k,F}$ FD-Indices are generated at node 7, as shown in Table 1, indicating fault at that node. Negative FD-Indices of very small magnitude, of the order of 10^{-5} or smaller, are generated at all other nodes, showing the fault discrimination capability of the APdSA protection algorithm.

When a fault occurs along a feeder, two FD-Indices (of $C_{k,P}$ or $C_{k,F}$) are generated at the two nodes at the ends of the feeder. The algorithm is able to identify a fault irrespective of fault type – whether single-phase to ground, three-phase to ground, phase-to-phase, or double-phase to ground. The fault indices are generated when (active) power flow imbalance is detected across a BAP zone, no matter the cause. The fault type can be determined from the phase units that operate for the particular fault. For example, a single phase-to-ground fault on the A-phase will generate a fault index on the element monitoring the A-phase only. A phase-to-phase fault will generate FD-Indices on the two faulted phases; no fault indices are detected on the healthy phase, as illustrated in Table 2 for a phase-to-phase fault along Feeder 10-11. The coupling between the phases has no impact on the algorithm since the algorithm is sensitive to active power flow imbalances only.

Node	$C_{k,P}$	$C_{k,F}$
5	−2.867E-05	−1.366E-06
6	−2.463E-05	−7.375E-07
7	0.660	2.971
8	−3.136E-05	−4.746E-05
9	−3.393E-05	−1.868E-09
10	−3.342E-05	−1.822E-09
11	−3.367E-05	−3.871E-06
14	3.740E-09	6.537E-09
21	−5.65E-05	−1.067E-05
23	−4.457E-05	−6.637E-09
27	−0.000	−1.628E-06
30	−8.570E-05	−0.000

TABLE 1. FD-Indices at selected nodes with single phase-to-earth fault at node 7 with $R_F = 3\ \Omega$.

	$C_{k,P}$	
Node	Faulted phase	Un-faulted phase
5	−7.491E-09	1.241E-10
6	1.322E-08	6.115E-10
7	−2.233E-08	−1.42E-09
8	1.747E-08	1.167E-09
9	−1.119E-08	−1.02E-09
10	0.429	−2.59E-09
11	0.426	2.887E-09
14	−8.756E-09	1.498E-10
21	2.4462E-11	−8.54E-12
23	−1.304E-08	−3.58E-10
27	−2.892E-09	1.357E-10
30	−2.833E-10	6.982E-11

TABLE 2. $C_{k,p}$ FD-Indices (in p.u.) for phase-to-phase fault at mid-point of Feeder 10-11.

2.3. Communication Requirements

The APdSA algorithm detects fault occurrence within a specific BAP zone. That is, FD-Indices appearing at a node simply indicate that a fault has occurred somewhere in the respective zone – meaning at the node or along one of the feeders in the zone. Subsequently, through peer-to-peer communications between the IED and those located at neighboring nodes, the protection algorithm is able to identify the specific faulted feeder in that zone. For example, when a fault occurs along Feeder 14-23, the positive FD-Indices generated at nodes 14 and 23 indicate fault somewhere in a region common to both Zone14 and Zone23 (Figure 1) which is the overlap zone represented by Feeder 14-23.

The relay at node 14, IED14, sends Request to Trip (RTT) signals to its neighboring IEDs at nodes 13, 14, 23 and 27. The IED at node 23 has also seen the fault (in

Zone23). It trips its CB (on Feeder 23-14) and sends a Permission to Trip (PTT) signal to IED14, which proceeds to trip its local CB on Feeder 14-23. This logic ensures that the correct faulted feeder, which is in the overlap zone of Zones 14 and 23, is isolated. The remainder of the IEDs at all the other nodes did not see the fault and their respective feeders are not tripped.

3. PERFORMANCE EVALUATION OF THE APDSA PROTECTION ALGORITHM

The theory underlying the APdSA fault detection algorithm may be described as abstract as it involves the formulation and use of some quantities that do not have physical meaning, or it is difficult to attach physical meaning to them. Performance evaluation based on analytical methods is therefore difficult. Modeling and simulations need to be used in order to transform the abstract formulations into visually identifiable quantities that can be easily understood. The simulations generate important results that are not apparent using an analytical approach. The performance of the APdSA protection algorithm is therefore evaluated through simulations using the Digsilent *PowerFactory* software.

A good relay operating principle permits tripping when called upon but blocks tripping when it is not required to. In order to evaluate the performance of the APdSA algorithm, the relay must be exposed to a set of disturbances [5] [27]. In the work reported in this paper, the disturbances include:

i. An in-zone fault which must trigger the relay.
ii. An out-of-zone fault which should not trigger the relay. That is, the relay must remain stable. The algorithm is differential in principle, but it is affected by external faults. The form of this response to external fault is important, especially for stability and selectivity evaluation.
iii. The exposures are extended to include fault resistance which can have an impact on the sensitivity of a relay. As the fault resistance increases, the relay sensitivity can be compromised.
iv. The protection should also be exposed to communication failure. The algorithm employs peer-to-peer communications between IEDs located at adjacent zones.

The speed of the relay measures the time between inception of fault and issuing of a tripping command by the relay. For time-current based protection, the speed is influenced by the time coordination requirements. However, for differential protection systems that see only "in-zone" faults, the speed depends on the measurement, communication, and computation load of the algorithm. As already discussed, the APdSA algorithm is differential in principle and no intentional delay needs to be introduced that might delay the triggering of the relay. However, the algorithm is subject to inherent latencies arising from the PMU measurement reporting delays, the propagation delay of the physical communication medium and the processing time of the algorithm [10].

4. RESULTS AND DISCUSSION

The modified IEEE 34 node test network was built in Digsilent *Powerfactory* software. A series of faults (in-zone and out-of-zone) of different fault resistances were simulated and the relay performance evaluated in terms of sensitivity, stability, speed, fault resistance and fault detection range.

4.1. APdSA Sensitivity

The algorithm must be sensitive to any fault occurring within its BAP zone. In this paper, the sensitivity is assessed by monitoring the magnitude of FD-Indices generated by fault in comparison to the fault pick-up threshold settings. As explained in Section 2.1, with appropriate placement of the PMUs, the load and generators can be excluded from the BAP zone. This means that changes to load and/or generation are not visible to the algorithm meaning ΔP_k in (2)-(3) is zero and appears only under fault conditions. The pick-up threshold for $C_{k,P}$ and $C_{k,F}$ can thus be set to zero.

When a fault occurs at the mid-point of a feeder, FD-Indices with magnitudes above the pick-up threshold settings (zero) are generated at the respective nodes, as discussed in Section 2.2. Of interest, though, are the FD-Indices generated at the un-faulted nodes. It can be seen from Tables 1-2 that when a fault occurs, the FD-Indices at most un-faulted nodes drop to negative values. At a few un-faulted nodes the FD-Indices have very small positive magnitudes of the order of 10^{-5} or lower. The pick-up threshold of $C_{k,P}$ and $C_{k,F}$ thus needs to be set slightly above zero, for example to a value that is of the order of 10^{-4}. As will become apparent in Section 4.5, this level of sensitivity allows the reach of the APdSA algorithm to extend to more than 95% of the protected feeder, over a wide range of fault resistances.

4.2. APdSA Stability

The APdSA algorithm must remain stable under external fault conditions. The stability is evaluated by monitoring the magnitude of the FD-Indices at nodes external to the

faulted zone. To demonstrate the stability of the algorithm, single phase to ground faults of 1 Ω resistance are simulated at several points external to Feeder 14-23 as shown in Table 3. Feeder 14-23 is located in the overlap region of Zone-14 and Zone-23 of the test network, as illustrated in Figure 1. The corresponding $C_{k,F}$ and $C_{k,P}$ FD-Indices generated at nodes 14 and 23 for the simulated faults are also given in Table 3. Analysis of this table shows that faults occurring at, for example, node 7 and along feeder 7-8 are not picked up by either IED at node 14 or 23, as indicated by the very small (below pick-up threshold) or negative magnitudes of the FD-Indices. A fault at node 8 is also not picked up as it lies on the boundary of Zone-23. However, faults along feeder 8-23 are picked up by the IED at node 23 as they are within Zone-23.

Similarly, faults at nodes 12, 13, and 15, and along feeders 12-13 and 15-16, are external to Zone-14 and are not detected. However, faults along feeders 13-14 and 14-15 are detected by the IED at node 14 as they are within Zone-14. But these are not picked up by IED at node 23 as they are external to Zone-23.

In short, the FD-Indices generated at nodes 14 and 23 due to out-of-zone faults move in the negative direction away from the pick-up thresholds. This drop to well below the pick-up thresholds eliminates any risk of out-of-zone tripping. That is, stability is assured for out-of-zone faults.

4.3. Selectivity and Speed

The results from Sections 4.1–4.2 show that the algorithm operates for fault within the respective BAP zone only. The algorithm does not see faults anywhere else. The APdSA algorithm is therefore highly selective in its operation, providing some kind of 'soft' unit protection. 'Soft' in the sense that the impact of a fault is also felt in external BAP zones but this results in negative or 'blocking' FD-Indices being generated. In conventional unit protection an external fault is not seen at all providing, in comparison, 'hard' unit protection.

The APdSA protection is thus able to achieve fast fault clearance times. The algorithm looks suitable for the modern and still evolving power system that incorporates numerous DGs and requires protection that is both fast and selective.

4.4. Impact of Fault Resistance

The impact of fault resistance on the fault detection is illustrated in Figure 3, which shows the variation of $C_{k,P}$ and $C_{k,F}$ with fault resistance. Figure 3a shows the FD-Indices detected by the IED at node 10 for a single-phase to ground fault at the mid-point of Feeder 10-11. Similar FD-Indices are detected by the IED at the remote end, node 11. It can be seen that detectable FD-Indices are generated over a range of fault resistances. The FD-Indices are relatively small for fault resistances approaching zero. However, the FD-Indices are relatively higher in the intermediate range. With the theoretical pick-up setting of zero, the relay can pick up faults with impedances of more than 1 kΩ. However, since a minimum pick-up slightly above zero needs to be set as discussed in Section 4.1, the actual fault resistance detection range may be reduced and faults of resistances higher than 1000 ohms may become difficult to detect, as evident from Figure 3b.

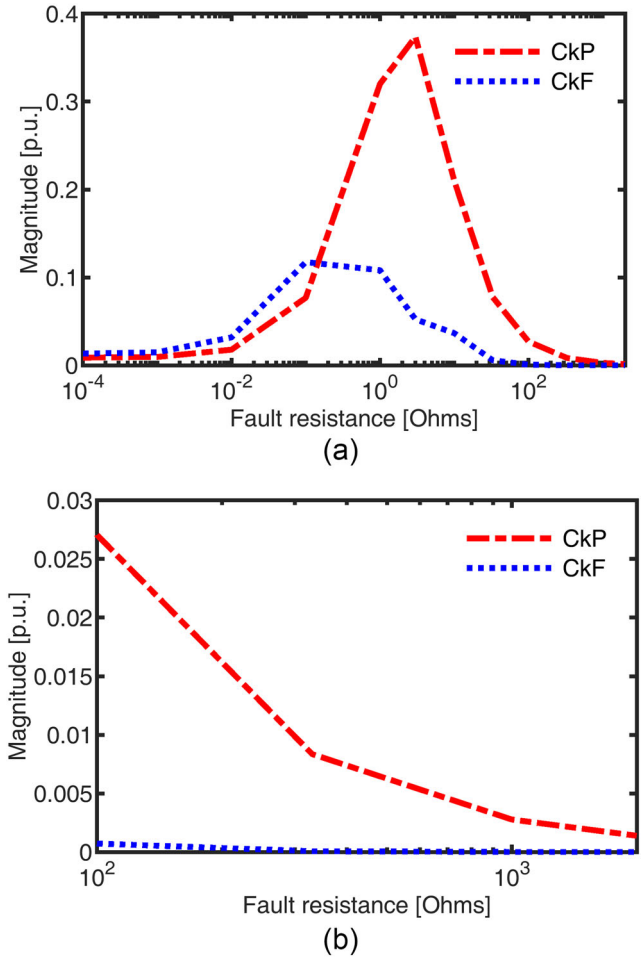

FIGURE 3. (a) Variation of FD-Indices (in p.u.) at node 10 with single phase-to-ground fault at mid-point of Feeder 10-11, (b) FD-Indices (in p.u.) at high fault resistances.

The FD-Indices generated at the two IEDs at nodes 10 and 11, for a phase-to-phase fault at mid-point of Feeder 10-11, are shown in Table 4. It can be seen that the

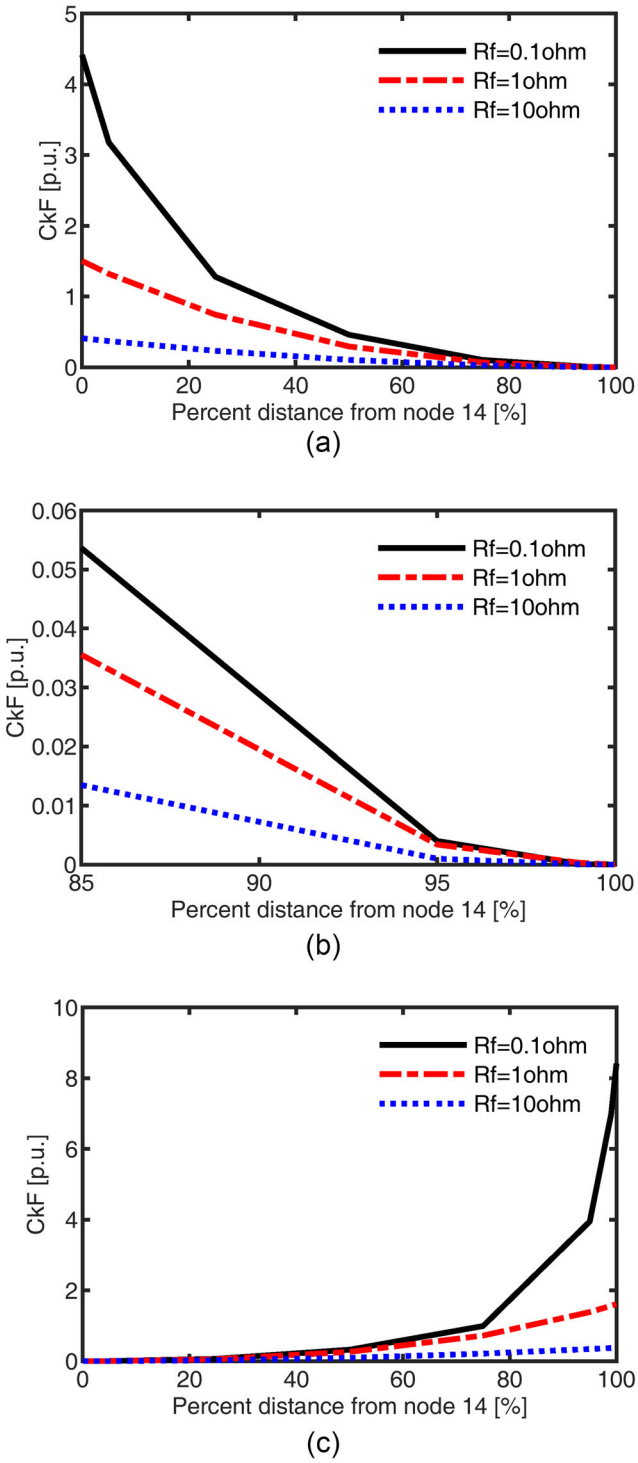

FIGURE 4. Variation of $C_{k,F}$ for single phase to earth faults at different locations along Feeder 14-23 measured from node 14: (a)-(b) $C_{k,F}$ detected at node 14 (c)-(d) $C_{k,F}$ detected at node 23.

algorithm is sensitive to faults over a range of fault resistances. Insignificant FD-Indices are generated on the healthy phase, as shown in Table 5.

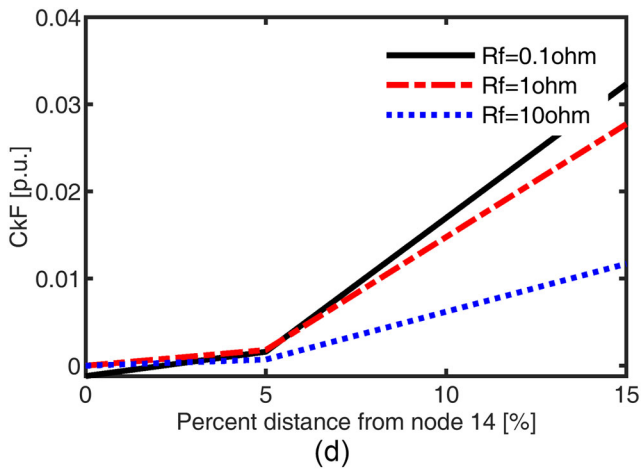

FIGURE 4. (Continued)

Fault position (R_F = 1 Ω)	$C_{14,F}$	$C_{14,P}$	$C_{23,F}$	$C_{23,P}$
Node 8	8.1E-09	1.9E-06	−7.7E-06	−0.003
Mid-point Fdr 8-23	1.7E-08	1.9E-06	0.267	0.667
Node 7	6.7E-09	1.4E-06	−5.0E-06	−0.002
Mid-point Fdr 7-8	3.4E-09	1.7E-06	−2.3E-06	−0.002
Node 13	3.9E-07	2.0E-06	−3.3E-05	−0.002
Mid-point Fdr 13-14	0.163	0.565	−3.5E-05	−0.003
Node 12	1.9E-07	1.9E-06	−2.7E-05	−0.002
Mid-point Fdr 12-13	2.7E-07	1.9E-06	−3.0E-05	−0.002
Node 15	2.2E-07	2.3E-06	−3.8E-05	−0.002
Mid-point Fdr 14-15	0.124	0.572	−4.4E-05	−0.002
Mid-point Fdr 15-16	1.9E-07	2.2E-06	−3.8E-05	−0.002

TABLE 3. $C_{k,F}$ and $C_{k,P}$ FD-Indices (in p.u.) for faults external to feeder 14-23.

4.5. Fault Detection Reach

The reach of the APdSA fault detection algorithm is illustrated in Figure 4, which shows the variation of $C_{k,F}$ detected by the IEDs at nodes 14 and 23, respectively, for single phase-to-ground fault of various resistances occurring at different distances along the Feeder 14-23, measured from node 14. Distances of 0% and 100% indicate fault at node 14 or 23, respectively. It can be seen that detectable FD-Indices are generated for faults occurring at distances up to 95% from the relay location. However, faults at the node itself are detected only by the IED at that node. The remote IED does not see this fault which, effectively, is at the boundary of its zone of protection. For example, for fault at node 14, the $C_{k,F}$ values generated at node 23 are very small (in fact, negative) and below the pick-up threshold. In this case, the busbar needs to be

	Fault resistance (ohms)					
	0	10^{-4}	1	10	100	1000
$C_{10,P}$	0.368	0.368	0.403	0.275	0.042	0.0044
$C_{10,F}$	0.022	0.022	0.002	0.028	0.000	1.0E-05
$C_{11,P}$	0.363	0.363	0.400	0.276	0.042	0.004
$C_{11,F}$	0.004	0.004	0.020	0.034	0.000	1.0E-05

TABLE 4. FD-Indices (in p.u.) with phase-to-phase fault at mid-point of feeder 10-11.

Fault resistance (ohms)					
	0	10^{-4}	1	10	100
$C_{10,P}$	4.0E-10	4.0E-10	4.0E-10	4.0E-10	4.0E-10
$C_{10,F}$	2.6E-19	2.6E-19	2.6E-19	2.6E-19	2.6E-19
$C_{11,P}$	−2.1E-10	−2.0E-10	−2.0E-10	−2.0E-10	−2.0E-10
$C_{11,F}$	−6.9E-20	−6.9E-20	−6.9E-20	−6.9E-20	−6.9E-20

TABLE 5. FD-Indices (in p.u.) on healthy phase with phase-to-phase fault at mid-point of feeder 10-11.

isolated by tripping all the local CBs. Faults close-up (within 5% range) to a node are also not seen by the remote IED. Since a busbar and close-up fault cannot be differentiated, inter-tripping is required to trip the remote CBs of that zone, effectively isolating the entire zone. However, successful re-closure may ensure quick restoration of supplies.

4.6. Impact of Communication Failure

The algorithm is distributed and involves peer-to-peer communications between neighboring nodes. The communication failure that must be considered in this context is that between any two neighboring IEDs. If the algorithm were to involve a centralized controller, then network-wide communication failure may need to be considered. In the distributed context, this would amount to loss of communication across all the peer-to-peer links. This scenario is not considered.

In the event of communication failure the IEDs should be able to use only locally available measurements to detect and isolate a fault. This scenario is tested for a fault along Feeder 15-28 of the test network. The peer-to-peer link between the IEDs at nodes 15 and 28 is lost. It is assumed that the local IED retains (in memory) the most recent measurements received from the neighboring nodes immediately before the loss of communication, meaning that the calculation of the FD-Indices at node k then uses the pre-fault voltages at the adjacent nodes and the post-fault voltage at node k.

$C_{k,F}$ FD-Index with extremely large magnitude of 17×10^3 (p.u.) was generated at nodes 15 in spite of the loss of communication. $C_{k,P}$ of negative magnitude of −48 (p.u.) was also generated. Similar $C_{k,F}$ and $C_{k,P}$ FD-Indices are generated at node 28. Hence, a fault can still be detected when communication has been lost between two neighboring IEDs. $C_{k,P}$ is negative in this particular case of phase-to-ground fault on line 15-28. However, further simulations indicate that $C_{k,P}$ may also take positive values for faults at other locations. But the $C_{k,F}$ is consistently positive with very large values for fault at any location. This means when loss of communication is detected, only $C_{k,F}$ should be used for detection of fault. In essence, the APdSA protection algorithm is tolerant to communication failure.

4.7. Comparison with Distance and Overcurrent Protection

The sensitivity and operating time of the APdSA relay to short circuit faults of varying fault resistance was compared to that of the conventional distance and overcurrent relays selected from the *PowerFactory* in-built models. The selected relay models are installed at Node 8 for protection of Feeder 7-8. The protection settings of the relays are given in Table 6. Only the zone 1 of the distance relay is included in the study. The results are given in Table 7. The results show that the APdSA relay can protect up to 95% of the protected line. However, as the fault resistance increases, the reach of the relay is reduced, as can be seen in Table 7. The phase element of the distance relay also fails to detect the high resistance faults when the impedance presented to the relay moves out of the relay characteristic, causing the relay to block.

The operating time of the APdSA relay is 5 ms and that of the distance relay model is 20 ms. The overcurrent elements operated according to the inverse time-current characteristics. The very long tripping times are due to the small fault current infeed from node 8 toward the fault, which is along Feeder 8-7 toward the main source/grid. The infeed is therefore being supplied by the DGs at nodes 27 and 30.

The 5 ms for the APdSA relay is only the processing time of the algorithm. To this should be added the phasor measurement and communication delays. Researchers in [28] developed a method for determining the end-to-end reporting latency of the PMU and the associated propagation and processing delays. The work reported a relay trip

Instrument Transformers		CT	750/1 A	VT	22/0.110 kV
APdSA		$C_{k,F}$ (p.u.)	0.002	$C_{k,P}$ (p.u.)	0.001
Distance	Phase	Relay reach (prim. Ω)	1.28	Relay Angle	70°
	Earth	Relay reach (prim. Ω)	3.86	Relay Angle	70°
Over-Current	Phase	PS	0.75	TMS	0.05
	Earth	PS	0.25	TMS	0.1

TABLE 6. Protection ratings and settings.

Fault resist-ance R_F	Fault Distance (From Node 8)	Operating Time (ms)				
		APdSA	Distance		Overcurrent	
			Phase	Earth	Phase	Earth
0.1 Ω	50%	5	20	20	485	443
	85%	5	20	20	501	453
	95%	5	20	20	515	464
	99%	5	–	20	518	466
	100%	–	–	20	520	466
3 Ω	50%	5	20	20	1465	606
	85%	5	20	20	2785	682
	95%	5	–	20	5369	715
	99%	–	–	20	6483	731
	100%	–	–	20	6852	735
10 Ω	50%	5	20	20	–	1242
	85%	5	20	20	–	1973
	95%	–	–	20	–	2531
	99%	–	–	20	–	2892
	100%	–	–	20	–	3002

Table 7. Node 8 Relay operating times for phase-to- phase-ground fault along Feeder 8–7.

time of less than 60 ms from fault inception for a current differential scheme employing PMU data transferred over a WAN. Researchers in [23] estimate wide area PMU reporting latency and communication time delay to be around 125 ms, considering a telephone line channel. From the above it can be seen that the proposed APdSA relay is still able to provide faster tripping than OC protection even if 125 ms delay is considered.

The distance relay uses single-point measurements and can thus determine fault condition quicker. However, delays are also introduced when communication is introduced to achieve permissive or blocking schemes, leading to distance relay operating times of up to 80 ms (processing and circuit breaker time) for the first zone and 500 ms for the second zone, as reported in [29].

5. CONCLUSION

This paper presented an evaluation of the performance of a voltage-based protection algorithm that uses power differential and sensitivity analysis to detect faults in active distribution systems. The algorithm operates over a protection zone that extends to include a busbar and all feeders terminating at that busbar. The results show that the algorithm is able to selectively differentiate between in-zone and out-of-zone fault. The algorithm can achieve this with high sensitivity, stability, and speed. The algorithm is thus unique in that it can concurrently improve the protection performance qualities of sensitivity, stability, selectivity and speed which traditionally have been shown to present conflicting requirements on the design of the protection. The algorithm is sensitive over a range of fault resistances and is tolerant to communication failure.

REFERENCES

[1] A. Grid, *Network Protection and Automation Guide*, 1st ed. United Kingdom: Alstom Grid, 2011,

[2] B. M. Weedy, B. J. Cory, N. Jenkins, J. B. Ekanayake and G. Strbac, *Electric Power Systems*, 5th ed. Chichester, West Sussex, United Kingdom: John Wiley, 2012.

[3] M. E. Valdes and J. J. Dougherty, "Advances in protective device interlocking for improved protection and selectivity," *IEEE Trans. Ind. Applicat.*, vol. 50, no. 3, pp. 1639–1648, 2014. May/June DOI: 10.1109/TIA.2013.2285941.

[4] M. H. Hairi and L. Haiyu, "Sensitivity and stability analysis of loss of main protection in active distribution networks," IEEE PES General Meeting | Conference & Exposition, National Harbor, MD, USA, 2014. in 27-31 July pp. 1–5.

[5] S. A. Saleh, R. Meng and R. McSheffery, "Evaluating the performance of digital modular protection for grid-connected permanent-magnet-generator-based wind energy conversion systems with battery storage systems," *IEEE Trans. Ind. Applicat.*, vol. 53, no. 5, pp. 4186–4200, September/October 2017. DOI: 10.1109/TIA.2017.2716381.

[6] T. P. Hinge and S. S. Dambhare, "Secure phase comparison schemes for transmission-line protection using synchrophasors," *IEEE Trans. Power Delivery*, vol. 30, no. 4, pp. 2045–2054, August 2015. DOI: 10.1109/TPWRD.2015.2417997.

[7] U. N. Khan and T. S. Sidhu, "A phase-shifting transformer protection technique based on directional comparison approach," *IEEE Trans. Power Delivery*, vol. 29, no. 5, pp. 2315–2323, October 2014. DOI: 10.1109/TPWRD.2014.2308898.

[8] F. Blaabjerg, Y. Yang, D. Yang and X. Wang, "Distributed power-generation systems and protection," *Proc. IEEE*, vol. 105, no. 7, pp. 1311–1331, Jul 2017. DOI: 10.1109/JPROC.2017.2696878.

[9] A. Roy and B. K. Johnson, "Transmission side protection performance with Type-IV wind turbine system integration," IEEE North American Power Symposium (NAPS), Pullman, USA, 2014. in 7-9 Sep. pp. 1–6.

[10] P. T. Manditereza and R. C. Bansal, "Protection of microgrids using voltage-based power differential and sensitivity analysis," *elect. Power Energy syst.*, vol. 118, pp. 105756, 2020. DOI: 10.1016/j.ijepes.2019.105756.

[11] P. T. Manditereza and R. C. Bansal, "Introducing a new type of protection zone for the smart grid incorporating distributed generation," Proceedings of the IEEE PES International Conference on Innovative Smart Grid Technologies (ISGT), Singapore, 2018. in 22-25 May pp. 86–90.

[12] P. T. Manditereza and R. C. Bansal, "Fault detection and location algorithm for DG-integrated distribution systems," *IET j. Engineering*, vol. 2018, no. 15, pp. 286–1290, 2018.

[13] IEEE Power & Energy Society. [Online]. https://ewh.ieee.org/soc/pes/dsacom/testfeeders/

[14] P. T. Manditereza and R. C. Bansal, "Multi-agent based distributed voltage control algorithm for smart grid applications," *Electric Power Components Syst.*, vol. 44, no. 20, pp. 2352–2363, 2016. DOI: 10.1080/15325008.2016.1219889.

[15] Q. Fu, A. Nasiri, A. Solanki, A. Bani-Ahmed, L. Weber and V. Bhavaraju, "Microgrids: Architectures, controls, protection, and demonstration," *Electric Power Components Syst.*, vol. 43, no. 12, pp. 1453–1465, March 2015. DOI: 10.1080/15325008.2015.1039098.

[16] A. Rathinam, S. Vanila and C. Harika, "Phasor measurement unit based wide area backup protection scheme for power transmission lines," *Energy Proc.*, vol. 117, no. 2017, pp. 1172–1181, 2017. DOI: 10.1016/j.egypro.2017.05.243.

[17] A. Miron, C. Popa, C. E. Bobric and M. Dragomir, "Considerations regarding implementing wide area monitoring, protection and control in north – east of Romanian power grid," 10th International Conference and Exposition on Electrical and Power Engineering (EPE2018), Iasi, Romania, 2018, in 18-19 October, pp. 0867–0872.

[18] I. Hall, et al., "New line current differential relay using GPS," IEEE Bologna PowerTech Conference, Bologna, Italy, 2003., in pp. 1–8.

[19] M. K. Neyestanaki and A. M. Ranjbar, "An adaptive PMU-based wide area backup protection scheme for power transmission lines," *IEEE Trans. Smart Grid*, vol. 6, no. 3, pp. 1550–1559, 2015. May DOI: 10.1109/TSG.2014.2387392.

[20] J. A. Jiang, J. Z. Yang, Y. H. Lin, C. W. Liu and J. C. Ma, "An adaptive PMU based fault detection/location technique for transmission lines Part I: Theory and algorithms," *IEEE trans. Power Delivery*, vol. 15, no. 2, pp. 486–493, April 2000.

[21] S. Affijulla and P. Tripathy, "A special protection scheme for transmission lines based on wide area monitoring system," IEEE 59th International Scientific Conference on Power and Electrical Engineering of Riga Technical University (RTUCON), Riga, Latvia, 2018, in 12-13 November, pp. 1–6.

[22] P. Kundu and A. K. Pradhan, "Power network protection using wide-area measurements considering uncertainty in data availability," *IEEE Syst. J.*, vol. 12, no. 4, pp. 3358–3368, 2018. November DOI: 10.1109/JSYST.2017.2721641.

[23] M. M. Eissa, M. E. Masoud and M. M. Elanwar, "A novel back up wide area protection technique for power transmission grids using phasor measurement unit," *IEEE Trans. Power Delivery*, vol. 25, no. 1, pp. 270–278, 2010. DOI: 10.1109/TPWRD.2009.2035394.

[24] J. Zare, F. Aminifar and M. Sanaye-Pasand, "Synchrophasor-based wide-area backup protection scheme with data requirement analysis," *IEEE Trans. Power Delivery*, vol. 30, no. 3, pp. 1410–1419, 2015. June DOI: 10.1109/TPWRD.2014.2377202.

[25] M. K. Jena, S. R. Samantaray and B. K. Panigrahi, "A new decentralized approach to wide-area back-up protection of transmission lines," *IEEE Syst. J.*, vol. 12, no. 4, pp. 3161–3168, December 2018. DOI: 10.1109/JSYST.2017.2694453.

[26] P. T. Manditereza and a R. C. Bansal, "Renewable distributed generation: The hidden challenges – A review from the protection perspective," *Renewable Sustainable Energy Rev.*, vol. 58, pp. 1457–1465, 2016. DOI: 10.1016/j.rser.2015.12.276.

[27] E. O. Schweitzer, III, B. Kasztenny, M. V. Mynam, A. Guzmán, N. Fischer and V. Skendzic, "Defining and measuring the performance of line protective relays," 43rd Annual Western Protective Relay Conference, Spokane, Washington, 2016, in October 18–20, pp. 1–21.

[28] S. M. Blair, M. H. Syed, A. J. Roscoe, G. M. Burt and J. P. Braun, "Measurement and analysis of PMU reporting latency for smart grid protection and control applications," *IEEE Access*, vol. 7, pp. 48689–48698, March 2019. DOI: 10.1109/ACCESS.2019.2903929.

[29] M. M. Eissa, "Resilient wide-area monitoring and protection scheme with IEEE Std. C37.118.1-2011 criteria for complex smart grid system using phase diagram," *IET Smart Grid*, vol. 2, no. 2, pp. 309–317, 2019. DOI: 10.1049/iet-stg.2018.0247.

BIOGRAPHIES

Patrick T. Manditereza received the BSc degree in electrical engineering from the University of Zimbabwe, Harare, in 1991 and the MSc in electrical engineering from the University of Bradford, United Kingdom, in 1997. He received the PhD in electrical engineering from the University of Pretoria, South Africa, in 2017. He was Protection Engineer with the Zimbabwe Electricity Supply Authority from 1991 to 1996 after which he joined the National University of Science and Technology, Zimbabwe, as lecturer and also consulted widely within the mining and electrical industries. He moved to the Polytechnic of Namibia, Windhoek, in 2004. Since 2006 he has been with the Central University of Technology Free State, Bloemfontein, South Africa. Dr. Manditereza is a registered Professional Engineer with the Engineering Council of South Africa. His research interests include the integration of renewable energy resources, protection of DG integrated networks, smart grids and microgrids, and low voltage DC power distribution.

Ramesh C. Bansal has more than 25 years of teaching, research & industrial experience. Currently he is Professor in the Department of Electrical and Computer Engineering at University of Sharjah, UAE. In previous postings he was with the University of Pretoria, South Africa, University of Queensland, Australia, Birla Institute of Technology and Science, Pilani, India; the University of the South Pacific, Fiji; and Civil Construction Wing, All India Radio. He has published over 300 papers in journals and conferences. Prof. Bansal is a Fellow, and CP Engg IET-UK, Fellow Engineers Australia, Fellow Institution of Engineers (India) and Senior Member-IEEE. He has diversified research interests in the areas of renewable energy and conventional power systems which includes wind, PV, hybrid power systems, distributed generation, grid integration of renewable energy, power systems analysis (reactive power/voltage control, stability, faults and protection), and smart grid.